Marine Pollution Bulletin 124 (2017) 480–487

Contents lists available at ScienceDirect

Marine Pollution Bulletin

journal homepage: www.elsevier.com/locate/marpolbul

Baseline

Characterization and source apportionment of polycyclic aromatic hydrocarbons (pahs) in the sediments of gulf of Pozzuoli (Campania, Italy)

Michele Arienzo[a,*], Carlo Donadio[a], Olga Mangoni[b], Francesco Bolinesi[b], Corrado Stanislao[a], Marco Trifuoggi[c], Maria Toscanesi[c], Gabriella Di Natale[c], Luciano Ferrara[c]

[a] Dipartimento di Scienze della Terra, dell'Ambiente e delle Risorse, Università degli Studi di Napoli Federico II, Largo San Marcellino 10, 80138 Naples, Italy
[b] Dipartimento di Biologia, Università degli Studi di Napoli Federico II, Complesso Universitario di Monte Sant'Angelo, Via Cintia 26, 80126 Naples, Italy
[c] Dipartimento di Scienze Chimiche, Università degli Studi di Napoli Federico II, Complesso Universitario di Monte Sant'Angelo, via Cintia 26, 80126 Naples, Italy

ARTICLE INFO

Keywords:
Polycyclic aromatic hydrocarbons
Bagnoli brownfield site
Marine sediments
Environmental geology
Diagnostic indexes

ABSTRACT

Most of the literature reports on the impact of the former Bagnoli brownfield on the pollution of Bagnoli Bay, embedded in the Gulf of Pozzuoli (GoP). Thus, we studied concentrations, types and sources of sixteen PAHs (EPA) in sediments at 22 sites along 5 transects covering the entire area of GoP. Outstanding levels of PAHs were found, varying from 7.1 μg g^{-1} to 2.5 E + 3 μg g^{-1}. Sediments collected at sites far away from Bagnoli were found to be polluted to a similar extent than those facing the brownfield site, with values > 100 μg g^{-1}. Total PAHs levels in the sediments of GoP were higher by thirty-eleven thousand fold than those reported by other studies from various marine sites in the world. Transit axes of fine and very fine sands and diagnostic indexes revealed a common pyrolytic PAHs pollution spreading from the Bagnoli plant to all GoP.

The contamination of Mediterranean Sea and of its coastland is of special concern due to the reduced circulation, the importance of oil traffic routes and the amounts of industrial inputs (Richir et al., 2015). Along the Southern Italian Mediterranean coast (Tyrrhenian Sea), the Gulf of Naples, GoN, is affected by the presence of several petroleum related industries, including refining, tankerage, military activities, and merchant and pleasure boating. In particular, the Gulf of Pozzuoli, GoP, in the northern sector of GoN, has been strongly impacted by the activity of brownfield site, ILVA of Bagnoli, which lasted almost one century. This was the second largest integrated steel plant in Italy, and is now under remediation by a Government project. Remediation started in 1996 and was extended to the coastal area marine sediments facing the brownfield site in 2001 (Albanese et al., 2010). The industries, originally sited in the Bagnoli area, included a smelting plant, a very large integrated steelwork (with blast furnaces, coke ovens, sinter plants, electric arc steel furnace), iron, coal and grain handling facilities, a factory which manufactured slate/fibre–cement roofing and cladding, and a cement works. Several studies (Bergamin et al., 2003; Romano et al., 2009; Albanese et al., 2010) have been carried out to evaluate the type, degree and extent of pollution by heavy metals, polycyclic aromatic hydrocarbons (PAHs), polychlorinated biphenyls (PCBs), total hydrocarbons (HC) and the ecological benthic assemblages in the stretch of sea facing the Bagnoli industry. High levels of PAHs and PCBs, well above the concentration levels permitted by the Italian law, were reported in the marine sediments of Bagnoli (Albanese et al., 2010). While PAHs and PCBs resulted of anthropic origin, metal contamination was proven to be mostly dependent on a natural hydrothermal enrichment process related to the volcanic activity of the Phlegrean Fields (PF) caldera, where many spas and geothermal springs occur (Albanese et al., 2010). To identify types of pollution that could be produced by these activities, a better understanding of sources generating polluting flows is necessary.

PAHs have been studied in different compartments of the environment, owing to their carcinogenic and mutagenic activities in living beings and/or humans (Lehr and Jerina, 1977). Because of their low vapor pressure, some PAHs are present in the air at ambient temperature, both as gas and associated with particles (Ravindra et al., 2008a, 2008b). The lighter PAHs, such as phenanthrene, are found almost exclusively in gas phase whereas the heavier PAHs, such as benzo[*a*] pyrene B[*a*]P, are almost totally adsorbed on to particles. Sixteen PAHs have been specified by the United States Environmental Protection Agency (EPA) as priority pollutants. Beside their harmful pattern, they have been intensively studied for their geochemical meaning as markers to identify origin of sedimentary deposits and evolution in aquatic environment (Soclo et al., 2000). Sources of PAHs in the environment include wastes from industrialized and urbanized areas, offshore petroleum hydrocarbons production or petroleum transportation. Each source, pyrolytic, petroleum and diagenetic hydrocarbons, originates

* Corresponding author.
E-mail address: michele.arienzo@unina.it (M. Arienzo).

http://dx.doi.org/10.1016/j.marpolbul.2017.07.006
Received 10 April 2017; Received in revised form 26 June 2017; Accepted 3 July 2017
Available online 08 July 2017
0025-326X/

characteristic PAHs patterns, therefore is possible to recognize processes generating the compounds. PAHs have different distribution patterns according to their production sources. Difficulties exist in identifying their origins in sedimentary deposits, owing to the possible co-existence of several sources (various pyrolytic sources, petrogenic contamination, early diagenesis). In addition, physical-chemical properties of some PAH, like chemical reactivity (photooxidation, oxidation), can contribute to modify the original distribution pattern of the emission sources (Butler and Crossley, 1981). In marine ecosystems, PAHs can undergo degradation by photooxidation in the superficial water layer (Mill et al., 1981), and by microbial activities into the sediments (Cerniglia and Heitkamp, 1989). However, the PAHs ubiquity in sediments indicates that accumulation phenomena dominate degradation processes in sedimentary matrices (Readman et al., 1984; Smith and Levy, 1990).

Despite this widespread applicability of PAHs, most studies were limited to a specific location or type of sample, with the result that few studies have comprehensively addressed the relative suitability of various commonly applied PAH ratios as indicators. Molecular indices based on PAH physical-chemical behavior covariability were developed to assess the various origins of these pollutants (Soclo, 1986; Baumard et al., 1998). By simultaneous association of various molecular indices, is possible to determine what process generated such hydrocarbons in the studied matrices (Lake et al., 1979; Budzinski et al., 1997).

Since most of the research has been concentrated on the stretch of sea facing Bagnoli, we considered of paramount importance investigate the real geographical mapping of PAHs distribution and sources along the entire GoP. The findings will help to formulate adequate pollutant control strategies since the site is also characterized by intensive commercial fishing which locally sustains an important industrial sector. Thus, to contribute to filling this gap, we expanded the area of study to the entire GoP by carrying out a stepwise research still in progress. The first phase, represented by this research carried out in 2016, concerned (i) the evaluation of rate pollution of sediments of GoP by 16 PAHs, (ii) their comparison with current regulations and previous studies and (iii) the selection of a limited set of PAHs ratios which exhibit the best potential to distinguish natural and anthropogenic sources. Perhaps of equal importance, this comprehensive PAHs dataset provides an opportunity to evaluate the consistency and completeness of PAHs source identification using ratios. We also determined sedimentary transit axes along the seabed by the data of grain size analysis. The axes, once mapped, were compared with the values of pollutants found in sediments in order to trace the zones of accumulation and dispersion for the different granulometric populations.

Research will continue to evaluate the sediment contamination by heavy metals, total hydrocarbons and their ecotoxicological assessment as well as chemical, physico-chemical, trophic and ecotoxicological characterization of sea water.

GoP is a large bay of the wider GoN, Fig. 1, sited on the Campanian Margin of the Tyrrhenian Sea and originated during a Pliocene extensional tectonic phase (Patacca et al., 1990; Sgrosso, 1998). Some 50 craters have been recognized both inland and offshore. Two main active volcanic districts, PF and Mt. Somma-Vesuvius have developed along the coast. The GoP represents the submerged sector of PF and is characterized by a central plain, with epiplastic sedimentation, delimited to the south by several submerged volcanic banks. Tectonics of PF is very dynamic: historical records of bradyseismic vertical movements date back to Greek colonization, over 2000 years BP. In 1583, a new mountain (Mt. Nuovo) beside the town of Pozzuoli was formed by a pyroclastic eruption within 48 h. Following the Naples earthquake of 23th November 1980, the ground uplifted with a rate of 3 mm per day due to positive bradyseismic movement (Damiani et al., 1987). Gas emissions (fumaroles), both on land (Solfatara Volcano) and underwater (Pozzuoli Bay), are also associated with volcanic activity. Underwater gas emission caused a yellow coloration due to colloidal sulphur and iron hydroxides in suspension as sedimentary particles (Colantoni, 1972). The Pozzuoli Bay (mean depth: ca 60 m, maximum depth: 110 m, Somma et al., 2016) has a surface area of 33 km^2 and a volume of approximately 2 km^3. Water exchange occurs between GoP and GoN through a section 2 km wide and 100 m deep (De Maio et al., 1982). The presence of submarine hydrothermal springs located along a NW–SE axis, in the eastern sector of the GoP (Sharp and Nardi, 1987), is clearly related to secondary volcanic activity of the PF and affects the natural chemistry of coastal marine waters, changing the evaluation of anthropogenic pollution. The fluids from these springs contain heavy and potentially toxic metals such as arsenic, mercury, copper, lead and cadmium. In contrast, hydrocarbons (mostly PAHs) are leached by rain fall percolating through soils and landfills contaminated by industrial activities. The sediment distribution in GoP is strictly correlated to climatic and tectonic events). Water circulation in the GoN is strictly related to the general circulation in the Tyrrhenian Sea (Carrada et al., 1980). Pennetta et al. (1998) recognize, during winter, a clockwise rotating circulation in the inner part of the gulf and a northward current offshore. Conversely, during summer, the inner circulation has an anticlockwise direction and the offshore current is towards the south. The contributions from inland determine an eutrophic coastal subsystem, that is conditioned by human activity. In particular, the GoP may be influenced by inputs from the Volturno River and the Naples harbour.

Sediments of the GoP were taken aboard the equipped boat identified as Antilia on December 2015 in 22 sites, Fig. 1 and Table 1, by a Van Veen grab along 5 transects, positioned on a coast-offshore alignment, perpendicular to the shoreline and all converging to the site 3_5, Fig. 1. Sample distribution was planned in order to have a good detail of the entire GoP, covering the highly anthropized area of Pozzuoli and Bacoli, Fig. 1, as well as the brownfield site of Bagnoli. Sea depth, measured with an ecograph, varies between 10 and 20 inshore up to 100 m deep offshore, and position of stations was determined by DGPS (Differential Global Positioning System), Table 1. Sediments were collected in plastic bags, wrapped in aluminium foil and sent in an ice box to the laboratory where they were frozen at − 20 °C.

Sediment samples were analysed for granulometric parameters, TOC, and PAHs (Tables 1, 3). The granulometric analysis was performed according to the usual techniques of sedimentology. Particularly, after preparation and washing with vacuum pump, all the samples were dried in an oven at 80 °C for 72 h, mechanically quartered, weighed with an analytical balance and subjected to dry sieving through a series of stacked sieves, with 1/4 ϕ class interval up to 63 μm, in a mechanical sieve shaker for 15′. Fractions from 63 to 2 μm were analysed through sedimentation in distilled water with 10% sodium oxalate at specific temperatures, according to Belloni (1969). For each sample histograms and cumulative curves were plotted (Blott and Pye, 2001), as well as calculated the granulometric fraction percentages (Table 1) and main statistical parameters, according to the graphic method of Folk and Ward (1957). Sediment dispersal along the seabed of Gulf of Pozzuoli was evaluated by a dedicated software (ArcMap version 10.2.2) with the aim to identify sedimentary transit axes (Barusseau, 1973; Cortemiglia, 1978a, 1978b, 1978c; De Pippo, 1989). Frequency curves for each sample were analysed and modal formulas, expressed by mode values and their percentage frequency of appearance, were recognized (Pauc, 1973; Long, 1975).

For TOC determination, samples of 0.5 g of ≤ 2000 μm dry sediments were weighed in ceramic vessels and analysed by a total organic carbon analyser, Skalar (The Netherlands). Sixteen PAHs indicated from Environmental Protection Agency (EPA) as important toxicological contaminants were determined: acenaphtene (ACE), acenaphthylene (ACY), anthracene (ANT), benzo(a)anthracene (BaA), benzo(b)fluoranthene (BbF), benzo(k)fluoranthene (BkF), benzo(ghi)perylene (BgP), benzo(a)pyrene (BaP), chrysene (CHR), dibenz(ah)anthracene (DhA), fluoranthene (FLT), fluorine (FLR), indene (IND), naphthalene (NAP), phenanthrene (PHE), pyrene (PYR). For the analysis of PAHs the IRSA CNR 25 method was followed and modified by replacing cyclohexane with acetone/n-hexane 1:1 v/v and using a longer sonication time of

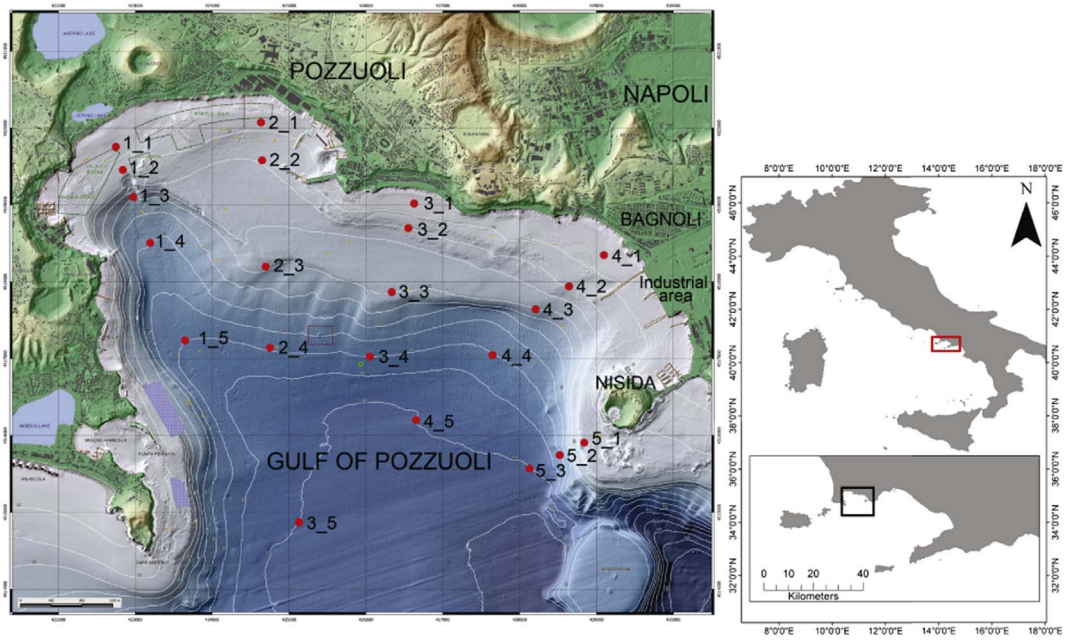

Fig. 1. Map of the sediment sampling in the Gulf of Pozzuoli. Depth is in meters bsl, coordinate system is WGS84 UTM Zone 33T (after Somma et al., 2016).

3 h by a ultrasonic disruptor, Brason (US), with a power of 300 W in pulser mode.

The extract (μL) was injected to a gas chromatograph (Shimadzu 2010 Plus, Japan) coupled with a mass spectrometer (MS-TQ8030-Shimadzu, Japan) and a fused silica HP5-MS capillary column (30 m × 0.25 mm i.d.) with film thickness of 0.25 μm (Agilent Technologies, US). High purity helium (99.9%) was used as carrier gas at a flow rate of 1.0 mL min^{-1}. The gas chromatograph was operated in splitless mode and separation was conducted with oven temperature programmed as follows: initial setting at 80 °C (2 min hold) ramped to 180 °C at 20 °C min^{-1} and finally to 300 °C at 5 °C min (9 min hold). The injector was held at 280 °C. The mass spectrometer was operated in scan mode and tuned with perfluorotributylamine (PFTBA) according to the manufacture criteria. Mass range *m/z* 50 and 300 were used for quantitative determinations. GC Solution software was used to obtain the chromatograms and for data calculations. An external calibration comprising of PAH standards was used to determine the identity and quantity of each component peak in sample chromatogram.

Samples were analysed in triplicate, for all the investigated points. The percentage of recovery was estimated by analysing 10 replicates of a fortified matrix, constituted by 13 PAHs at a known concentration. The range of the recovery percentage was 57–130%, in accordance with current methods normed. A good PAHs cleanup separation technique with minimum interference of coextract that may influence the accuracy of the result was obtained, indicating good selectivity and specificity of the method.

The detection limit (LOD) and limit of quantification (LOQ) were calculated using the range method of prediction to 95% of linear regressions, for each investigated PHAs. The calculated average values of LOD and LOQ were 0.1 and 0.3 μg g^{-1}, respectively. The quality of the

Table 1
Sampling locations associated to water depts., total organic carbon (TOC) and grain size of sediments from Pozzuoli Gulf.

Sampling stations	Latitude (N)	Longitude (E)	Depth (m)	TOC %	Gravel %	Sand %	Silt %	Clay %	Class[a]
1_1	40°49′27.55″N	14°5′2.94″E	8.0	1.34	4.68	94.94	0.33	0.05	Fine sand
1_2	40°49′16.89″N	14°5′8.74″E	24.8	1.51	1.59	97.29	0.96	0.16	Fine sand
1_3	40°49′6.81″N	14°5′15.07″E	45.1	3.27	35.26	60.35	4.1	0.29	Medium sand
1_4	40°48′49.34″N	14°5′31.38″E	58.6	1.72	33.74	61.71	4.36	0.19	Coarse sand
1_5	40°48′10.61″N	14°5′58.29″E	80.0	1.59	0.35	84.33	14.4	0.92	Very fine sand
2_1	40°49′41.34″N	14°6′19.46″E	8.0		0.69	99.31	–	–	Coarse sand
2_2	40°49′23.95″N	14°6′21.93″E	25.8	1.84	1.5	97	1.4	0.1	Very fine sand
2_3	40°48′42.91″N	14°6′29.06″E	34.0	0.98	6.72	91.81	1.32	0.15	Fine sand
2_4	40°48′6.96″N	14°6′39.17″E	72.5	1.4	4.18	85.91	9.3	0.61	Very fine sand
3_1	40°49′5.98″N	14°7′50.41″E	7.5	0.09	0.67	99.33	–	–	Medium sand
3_2	40°48′53.02″N	14°7′46.26″E	23.8	0.64	5.1	94.9	–	–	Fine sand
3_3	40°48′33.38″N	14°7′38.47″E	38.0	1.17	2.89	96.11	0.88	0.12	Fine sand
3_4	40°48′2.54″N	14°7′28.73″E	75.3	1.66	0.83	89.01	9.71	0.45	Very fine sand
3_5	40°46′59.22″N	14°7′6.01″E	100.0	1.65	2.35	83.91	13.28	0.46	Very fine sand
4_1	40°48′46.43″N	14°9′30.87″E	7.7	9.2	0.06	99.94	–	–	Fine sand
4_2	40°48′32.74″N	14°9′17.63″E	21.5	2.6	0.57	98.89	0.47	0.07	Fine sand
4_3	40°48′20.83″N	14°9′5.43″E	47.8	10.05	6.89	67.12	25.86	0.13	Very fine sand
4_4	40°48′6.92″N	14°8′49.11″E	71.5	4.28	9.42	68.15	21.68	0.75	Very fine sand
4_5	40°47′33.22″N	14°8′11.91″E	98.0	2.17	1.87	93.54	4.29	0.3	Fine sand
5_1	40°47′33.96″N	14°9′28.91″E	22.7	0.34	49.15	50.85	–	–	Very fine gravel
5_2	40°47′29.99″N	14°9′17.74″E	47.8	0.12	0.29	99.07	0.52	0.12	Fine sand
5_3	40°47′24.71″N	14°9′0.89″E	91.0	2.44	0.23	87.99	11.37	0.41	Very fine sand

[a] Classification of grain size sediment (Folk and Ward, 1957).

Table 2
Range of mode values, modal peaks and frequency percentages of appearance of the five granulometric sub-populations in sediments.

Sub-population	Mode (mm)	Modal peak (mm)	Appearance (%)
Very coarse sand	0.853–0.853	-[a]	4.54
Coarse sand	0.0755–0.603	0.151	9.09
Medium sand	0.0755–0.302	0.302	9.09
Fine sand	0.0755–0.213	0.151	40.90
Very fine sand	0.0755–0.0755	-[a]	36.36

[a] Undefined modal peak.

analytical results is assured by participation in ring tests for the determination of PAHs from sediments and similar matrices. Based on grain size, the sediments of GoP, Table 1, were mostly sandy with sand content ranging from 50.85% at 5_1 to 99.94% at 4_1. However, it is interesting to note how the sediments result more silty offshore, with peak up to 25.86% at the middle portion of the transect 4 facing the brownfield site. Along the littoral shelf, sediments ranged from coarse sand to sandy silt. They partly represent relic deposits of ancient beach. The coarse fraction is constituted of bioclastic and pumiceous elements (De Pippo et al., 2002). The clay content of these sediments is < 1.0%. TOC values ranged from 0 to 10.0% at 2_1 and 4_3, respectively, with values > 2.0% along entire transect 4, whereas this threshold was surpassed only at discrete points of transect 1, 3.27% at 1_3, and transect 5, 2.44% at 5_3. The highest TOC contents at transect 4 were expected because it is located near the Bagnoli brownfield site. No significant relationships was found between sediments sizes and TOC ($p = 0.03$).

The analysis of modal formulas of the 22 samples and their frequency of appearance, allowed to identify granulometric subpopulations which contribute to sedimentary dynamics of the study area, Table 2. The following modal average formula was obtained:

$$(?)\ 4.54\% + (0.151)\ 9.09\% + (0.302)\ 9.09\% + (0.151)\ 40.90\% + (?)\ 36.36\% \quad (1)$$

Questions marks in (1) indicate undefined modal peaks due to mode equal values.

Table 2 and formula (1) show that granulometric subpopulations which effectively contribute to sedimentary dynamics of study area are the fine sand, and secondarily the medium and coarse sand. In order to recognize features of drift of marine sandy sediments along the coast and seaward, maps of transit axes of the recognized subpopulations were drawn, including that of very fine sand, Fig. 2, which are normally more polluted. In particular, transit axes of very fine sand, a fraction with high frequency of appearance, Table 2, were constructed also considering the increasing percentages of granulometric fraction from the inshore dispersal zones towards the offshore accumulation zones related to seabed morphology. Map of transit axes of the fine sand, Fig. 2a, shows a prevailing littoral drift westward due to longshore currents, within 10 m depth in the central sector of the gulf. An aliquot of sediment moves towards the southwest and south, according to an anticlockwise cell circulation, depositing between 30 and 40 m depth along a large marine terrace. Instead, part of sediment not far from the northern pier of former steel industry at Bagnoli, drifts in NE-SW direction along a transverse incision, between 20 and 80 m depth, then accumulates to about 90 m depth. A smaller amount of sediment moves to the southeast, parallel to the coast, depositing on a marine terrace at 30 m depth near Nisida Island.

Map of transit vectors of very fine sand, Fig. 2b, shows that sediment dispersal is connected to offshore currents. From the shelf, these sediments move transversely along an incision of the slope, with head to about 40 m. Then, sediments shift to the west along the base of slope at 80 m depth, due to contour currents, and accumulate to the south at about 90 m depth, at the end of a westernmost incision. An aliquot of sediments drifts to the southeast towards Nisida Island depositing down to 90 m depth. Briefly, while the fine sand tends to move more inshore and westward respect to brownfield site, the very fine sand has a prevailing transit axis more offshore, mainly E-W oriented respect to the same site, spreading over the entire extension of GoP. Summarizing, marine sediments within 15 m depth show a littoral drift based on clockwise cell circulation, already desumed by the analysis of their distribution, due to E-W oriented longshore currents and rip currents towards southwest, according to De Pippo et al. (2002). Sediments over 20 m deep move along two main transversal incisions located at the edge of gulf, with a NE-SW and NW-SE direction and from 2 to 4 km long, respectively. Finally, these deposits accumulate to about 90 m depth. Both paleo-channels, modeled on the mainland by streams in the Late Quaternary and submerged during postglacial sea-level rise, play a significant morphological control on dispersal of marine sediment offshore (De Pippo et al., 2004) and are featured by paleo-alluvial fans at the base.

Table 3 reveals outstanding levels of PAHs over the entire GoP with a range of total PAHs from 7.1 $\mu g\ g^{-1}$ at 3_1, near the coastline and 7.5 m depth, to 2.5 E + 3 $\mu g\ g^{-1}$ at 4_3, along the transect facing the brownfield site of Bagnoli and 47.8 m depth. Table 3 also shows the individual concentrations of priority dangerous PD PAHs: NAP, ANT, BbF, BkF, BaP and BgP and their total values. These latter ranged between 2.7 $\mu g\ g^{-1}$ at 2_1 and 8.5 E + 2 $\mu g\ g^{-1}$ at 4_3 being thirteen and more than four thousand fold the legal limit of 0.20 $\mu g\ g^{-1}$. These data

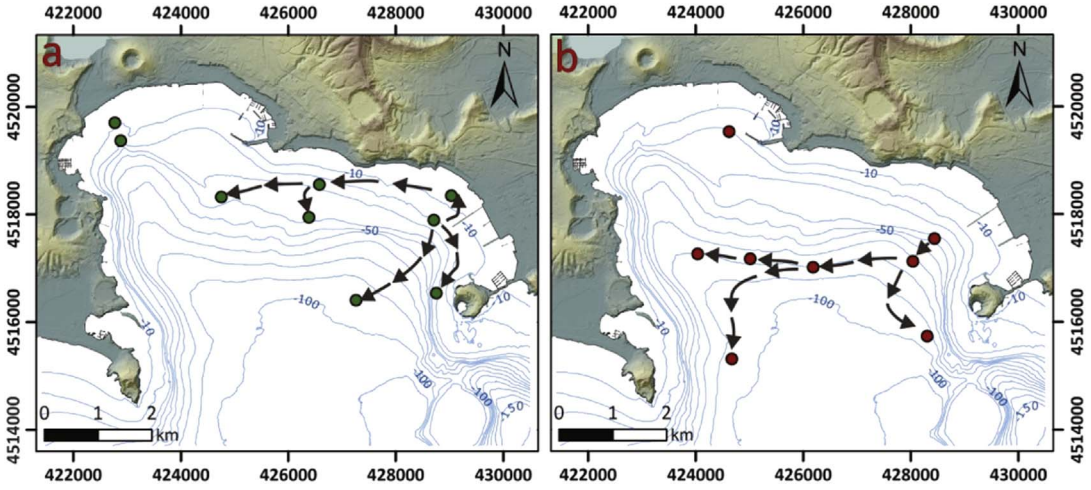

Fig. 2. Mobilization of marine sediments in the Gulf of Pozzuoli based on modal analysis: transit axes of (a) fine sand and (b) very fine sand. DTM Lidar basemap by MATTM - Environmental Remote Sensing Plan (PT-A). Depth is in meters bsl, coordinate system is WGS84 UTM Zone 33T.

Table 3
Concentrations of individual PAHs in the sediments (μg g^{-1}).

Stations	ACE	ACY	ANT	BaA	BbF	BkF	BgP	BaP	CHR	DhA	FLT	FLR	IND	NAP	PHE	PYR	Total PAH	Total PD[a] PAH
1-1	0.38	0.56	0.56	1.5	2.4	1.2	0.78	0.80	1.4	0.81	2.3	0.40	0.95	0.40	0.82	1.9	17	6.1
1-2	0.44	0.99	1.9	3.2	7.4	2.9	1.4	6.7	3.5	0.67	9.4	0.55	1.9	0.49	3.3	6.9	52	21
1-3	0.48	0.82	1.1	2.1	5.1	2.0	4.6	4.5	2.2	1.3	5.0	0.53	6.0	0.68	1.9	3.9	42	18
1-4	3.0	9.7	15	51	62	22	30	44	53	9.5	1.5 E + 2	7.7	40	3.5	17	1.3 E + 2	6.4 E + 2	1.8 E + 2
1-5	0.71	1.5	2.4	5.8	22	8.2	4.9	25	6.4	1.4	14	0.86	5.6	1.6	4.6	10	1.1 E + 2	64
2-1	0.025	0.025	0.36	0.025	0.025	0.025	1.6	0.63	0.68	0.77	0.41	0.025	1.8	0.025	0.36	0.43	7.2	2.7
2-2	3.0	5.8	8.2	16	23	9.1	13	17	16	6.3	38	6.8	16	3.6	13	31	2.3 E + 2	74
2-3	0.33	0.70	1.4	3.0	4.1	1.5	2.2	22	2.8	0.85	6.8	0.78	3.0	0.50	2.5	5.3	58	32
2-4	0.75	2.1	3.3	6.1	7.7	2.8	4.3	5.8	5.5	1.3	13	1.4	5.6	1.6	6.0	11	78	25
3-1	0.025	0.025	0.36	0.67	0.68	0.37	0.63	0.68	0.34	0.55	0.76	0.025	0.67	0.025	0.56	0.67	7.1	2.8
3-2	0.29	0.56	1.5	3.5	4.4	1.5	2.3	3.1	3.2	0.89	8.1	0.74	3.1	0.30	2.4	6.1	42	13
3-3	0.39	0.95	1.6	3.1	4.2	1.5	2.3	2.9	3.0	0.89	7.7	0.85	3.0	0.76	2.7	6.0	42	13
3-4	1.1	2.9	4.1	8.5	12	4.5	6.7	8.4	8.2	1.9	19	1.6	8.0	3.4	6.8	15	1.1 E + 2	39
3-5	0.52	1.3	2.1	4.2	6.0	2.0	3.2	4.0	4.1	1.1	10	1.1	4.3	1.3	4.2	7.7	57	19
4-1	10	25	35	58	78	30	40	57	56	11	1.7 E + 2	16	50	9.9	60	1.4 E + 2	8.4 E + 2	2.5 E + 2
4-2	1.0	2.9	6.1	9.3	12	4.3	6.8	8.7	8.7	1.8	25	1.9	7.6	1.5	10	19	1.3 E + 2	39
4-3	23	55	1.0 E + 2	1.9 E + 2	2.6 E + 2	94	1.6 E + 2	1.8 E + 2	1.9 E + 2	34	3.9 E + 2	46	1.9 E + 2	47	2.3 E + 2	3.3 E + 2	2.5 E + 3	8.5 E + 2
4-4	4.1	8.5	15	36	58	21	30	41	38	11	75	6.9	40	9.0	27	61	4.8 E + 2	1.7 E + 2
4-5	1.3	3.1	4.9	8.9	12	4.4	6.4	8.7	8.6	2.0	20	2.4	7.6	4.2	9.3	16	1.2 E + 2	41
5-1	0.37	0.57	0.92	1.2	1.4	5.7	0.96	1.2	0.91	0.62	2.6	0.74	1.2	0.37	1.6	2.0	17	5.4
5-2	0.29	0.46	0.40	0.76	0.86	0.45	0.72	0.80	0.44	0.58	1.0	0.67	0.88	0.40	0.72	0.89	10	3.6
5-3	5.1	9.7	16	30	41	15	22	29	30	8.4	73	9.4	28	6.7	32	58	4.1 E + 2	1.3 E + 2
Law limits[b]			45 E-3		40 E-3	20 E-3	55 E-3	30 E-3			110 E-3		70 E-3	35 E-3				200 E-3

[a] PD: priority dangerous: NAP, ANT, BbF, BkF, BaP, BgP according to the rules of the law nr. 219/2010.
[b] DM 14 April 2009, nr 56.

stressed how the greatest pollution levels were found along transect 4 in front of the industrial site, where levels do not fall below ~35 μg g^{-1}. What was surprising was that the sediments collected at 1_4 and 5_3, quite far away from the potential emitting PAHs source of Bagnoli, were found to be polluted to a similar extent than the transect 4 with values > 100 μg g^{-1}. Furthermore, not too far away from transect 5 and beyond Cape Miseno, PAHs concentrations were at negligible levels (Mangoni et al., 2016). Thus, our data largely surpassed the upper limit (> 5 μg g^{-1}) of the four categories of PAH pollution classification reported by Baumard et al. (1998), hence all the sediments of the GoP can currently be considered heavily polluted with PAHs.

A very significant correlation was found between the concentration of total PAHs and the concentrations of TOC (r = 0.85). Strong correlations between total PAHs and TOC are reported by Simpson et al. (1996) when the total PAH concentration is > 2 μg g^{-1}, which sustains the high correlation found in our study. PAHs are highly hydrophobic and usually accumulate in the sediment with high TOC content (Dahle et al., 2003).

To evaluate if the sediment contaminated by PAHs in GoP (7.1 μg g^{-1} − 2.5 E + 3 μg g^{-1}) will have a toxic effect (Long et al., 1995), the total PAHs were also compared against effects-based guideline values such as effects range-low, ERL, and effects range-median, ERM. The concentrations of total PAHs were much higher than the sediment quality guidelines (SQGs) for the ERL of 4.0 μg g^{-1} at all the studied stations whereas surpassed the ERM limit of 45 μg g^{-1} at most of the study sites (64%). These findings suggest that the sediments across the overall GoP were toxic to the organisms. The total PAHs concentrations in the sediments of GoP were higher by thirty-eleven thousand folds than those reported by other studies from various marine sites in the world (Nasher et al., 2013). The dominant PAH compounds found in the sediment samples include FLT (47 μg g^{-1}), PYR (39 μg g^{-1}), BbF (28 μg g^{-1}) and BaP (22 μg g^{-1}) with a content percentage of 16, 12, 10 and 9.8% of the total PAHs in all stations, respectively. The amounts of FLT, PYR and BaP were higher than their respective ERL and ERM SGQs values: FLT 0.60–5.1 μg g^{-1}, PYR 0.66–2.6 μg g^{-1}, BaP 0.43–1.6 μg g^{-1}. These results indicate that the probability of a positive toxic effect is higher than 50% and hence organisms, especially fish in this location, are in dangerous conditions. Table 3 indicates outstanding levels of individual PAHs in all GoP with mean values higher than law limits from one hundred twenty seven fold (NAP) to seven hundred twenty five fold (BaP). Benzo(a)pyrene (BaP) is considered as the most hazardous of the seven carcinogenic PAHs (Wang et al., 2010). An effective marker of pollution by BaP was detected in all sediment samples where the concentration ranged from 0.63 to 1.8 E + 2 μg g^{-1} (mean of 22 μg g^{-1}).

The percentage contribution of each individual PAH to ΣPAHs is depicted in Fig. 3a. As shown, in almost all samples IND, FLT, PYR, BbF, BaP and BgP accounted for > 5% of ΣPAHs, with peaks of 24% for IND at 2_1 and 38% for BaP at 2_3. FLT and BgP also reach high presence ~23% at 1_4 and 2_1, respectively. The composition pattern of PAHs by ring size in the sediment samples of GoP is shown in Fig. 3b. On average, the high molecular weight (HMW) PAHs with 5,6 rings (BbF, BkF, BaP, DhA, BgP) and 4 rings (FLT, PYR, BaA, CHR) account for 33 and 42% of the total PAH concentrations, respectively. However, the lower molecular weight (LMW) PAHs with 2,3 rings (IND, NAP, ACY, ACP, FLR, PHE, ANT) comprised the 25% of the total PAH concentrations. The results indicate that the high content of HMW fractions may be due to low water solubility, less volatility and higher persistence of the HMW compared with the LMW in an aquatic environment (Zakaria and Azril Mahat, 2006). The major source of HMW-PAHs in this area is probably anthropogenic. However, the high abundance of LMW-PAHs in some stations such as 2_1 suggests a relatively recent local PAH sources that entered the sea water (Law et al., 1997). The results of the paired sample *t*-test of the LMW to HMW-PAHs (p = 0.05) and the correlation coefficient between LMW and HMW was significant and positive (R = 0.99), suggesting same inputs for both LMW and HMW.

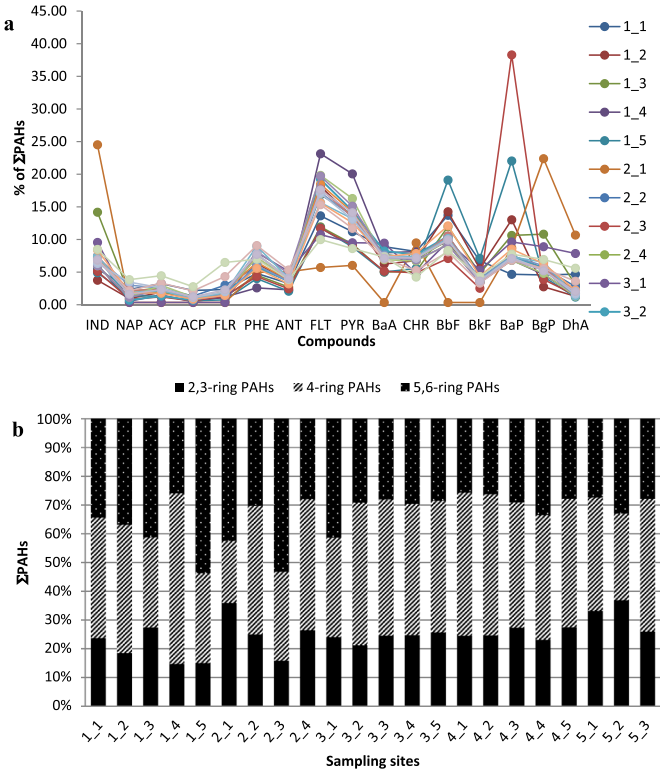

Fig. 3. A relative concentration in percentage of individual PAHs and different categories PAHs to ΣPAHs: a) individual PAHs; and b) two- to six-ring PAHs at each site.

Diagnostic ratios and statistical analysis are used to explain the details regarding the sources of PAHs in sediment samples.

Several PAH diagnostic ratios have been selected as indicators to distinguish between petrogenic and pyrogenic sources. Table 4 shows twelve diagnostic indexes and the reference values to establish the PAHs possible sources. The indexes split into two main groups: one where pyrogenic PAHs are related to total or to light PAHs pool and the other where the less thermodynamically stable PAH isomers are related to the more stable ones. These values were compared with those determined at each individual sampling station, Table 5. The ratios of all the indexes suggest that the PAHs are from a combustion source, including the ratio ANT/(ANT + PHE) which is reported by Yunker et al. (2002) as the most frequently used in distinguishing between combustion and petroleum sources. The ratio > 0.1 indicates a dominance of combustion. Yunker et al. (2002) also suggested that FLT/(FLT + PYR) > 0.5, as in our case, Table 5, implies combustion of coal. When plotting ANT/(ANT + PHE) vs. FLT/(FLT + PYR), Fig. 4a, it is clearly demonstrated that, with the exception of the site 2_1, PAHs derived from combustion source. To assess contamination sources PHE/ANT was plotted against FLT/PYR, Fig. 4b. Two matrices, a petroleum and a coal tar, typical of, respectively, petrogenic and pyrolytic fingerprints, are included in the graph. Most of samples are grouped and are characterized by FLT/PYR values > 1 and PHE/ANT values < 8, which is characteristic of strong pyrolytic input. In the same way plotting BaA/(BaA + CHR) vs. FLT/(FLT + PYR), Fig. 4c, also evidenced the pyrogenic source of the studied (Tobiszewski and Namiesnik, 2012) except for site 2_1 of petrogenic origin. In the end even the LMW/HMW ratio (sum of the low molecular weight PAH concentrations versus sum of the higher molecular weight PAH concentrations) evidenced the predominance of pyrogenic contamination.

Data seam to reveal that the main contribution source of PAHs in the GoP arises by the carbon fossil distillation (about one hundred year of plant operation) inside the Bagnoli brownfield site and direct dry and wet deposition in the sea as well as all round the plant. On the basis of a theoretical density value for sediments of 2.5 g cm^{-3}, a sampling depth of 10 cm and a surface of GoP of 33 km^2, we estimated a mass of total PAHs of ~2260 t, corresponding to an input from the brownfield site of 25 t $year^{-1}$, which is largely underestimated respect to the real daily emission rate because of degradation phenomena and land deposition of PAHs. This annual emission of PAHs is not too far from PAHs emission reported for the steel plant of Taranto, Italy, 32.2 t $year^{-1}$, (ISPRA, 2009) which is known as the largest in Europe.

When the principal component analysis (PCA) is applied, and average concentrations of 16 PAHs as active variables and 22 sites as subjects were selected, the normalized PAH data distributed respect to

Table 4
Source indicators and their respective diagnostic ratios.

Ratios	Petrogenic[l]	Petroleum burning/vehicular emission	Coal combustion	Softwood combustion	Pyrogenic	Aluminium smelter emissions
PHE/ANT[a]	> 15				< 10	
FLT/PYR[b]	> 1				≤ 1	
CHR/BaA[c]	> 1				< 1	
LMW/HMW[d,m]	> 1				< 1	
ΣCOMB/ΣPAHs[e]	< 1				~1	
BbF/BkF[f]						2,5–2,9
BaP/BgP[g]		> 0.6				
ANT/(ANT + PHE)[h]	< 0.10	> 0.10	> 0.10	> 0.10	> 0.10	
FLR/(FLR + PYR)[i]	< 0.5					> 0.5
FLT/(FLT + PYR)[j]	< 0.40	0.40–0.50	> 0.50	> 0.50	> 0.40	
BaA/(BaA + CHR)[k]	< 0.20	> 0.35	0.20–0.35	> 0.35	> 0.35	
Ring456/TPAS[m,n]	< 0.40	> 0.50	> 0.50	> 0.50	> 0.50	

[a] Soclo (1986).
[b] Sicre et al. (1987).
[c] Parlanti (1990).
[d] Soclo et al. (2000).
[e] Ravindra et al. (2008a).
[f] Hwang and Foster (2006).
[g] Tobiszewski and Namiesnik (2012).
[h] Pies et al. (2008).
[i] Ravindra et al. (2008b).
[j] De La Torre-Roche et al. (2009).
[k] Akyüz and Çabuk (2010), Yunker et al. (2002).
[l] Yan et al. (2004).
[m] LMW: PHE, ANT, FLT, PYR. HMW: BaA, CHR, BbF, BkF, BaP, BgP, DhA.
[n] Ring456: Total 4–6 ring PAHs (mainly originated from combustion); ΣCOMB (FLT, PYR, BaA, CHR, BbF, BkF, BaP, BgP); ΣPAHs sum of total PAHs.

Table 5
Diagnostic ratios determined at each individual sampling station.

Stations	PHE/ANT	FLT/PYR	CHR/BaA	LMW/ HMW	ΣCOMB/ ΣPAHs	BbF/BkF	BaP/BgP	ANT/ (ANT + PHE)	FLR/(FLR + PYR)	FLT/ (FLT + PYR)	BaA/ (BaA + CHR)	Ring456/ TPAS
1-1	1.5	1.2	0.92	0.64	0.72	2.0	1.0	0.41	0.17	0.55	0.52	0.76
1-2	1.7	1.4	1.1	0.83	0.80	2.6	4.7	0.37	0.07	0.58	0.48	0.81
1-3	1.7	1.3	1.0	0.55	0.70	2.5	0.98	0.37	0.12	0.56	0.50	0.73
1-4	1.1	1.1	1.0	1.1	0.84	2.8	1.5	0.47	0.06	0.54	0.49	0.85
1-5	1.9	1.3	1.1	0.42	0.84	2.7	5.1	0.34	0.08	0.57	0.47	0.85
2-1	1.0	0.9		0.42	0.54		0.39	0.50	0.00	0.49		0.65
2-2	1.6	1.2	0.97	0.91	0.72	2.5	1.3	0.38	0.18	0.55	0.51	0.75
2-3	1.8	1.3	0.95	0.44	0.83	2.8	9.9	0.36	0.13	0.56	0.51	0.84
2-4	1.8	1.2	0.90	1.0	0.72	2.8	1.3	0.35	0.11	0.55	0.53	0.74
3-1	1.6	1.1	0.51	0.60	0.69	1.8	1.1	0.39	0.00	0.53	0.66	0.77
3-2	1.5	1.3	0.93	0.95	0.77	2.9	1.3	0.39	0.11	0.57	0.52	0.79
3-3	1.7	1.3	0.98	1.0	0.73	2.8	1.3	0.37	0.13	0.57	0.51	0.75
3-4	1.7	1.3	0.96	0.91	0.74	2.6	1.2	0.37	0.09	0.56	0.51	0.75
3-5	2.0	1.3	0.97	0.98	0.72	3.0	1.3	0.34	0.12	0.57	0.51	0.74
4-1	1.7	1.2	0.97	1.2	0.74	2.6	1.4	0.37	0.10	0.55	0.51	0.75
4-2	1.7	1.3	0.93	1.2	0.74	2.7	1.3	0.37	0.09	0.57	0.52	0.75
4-3	2.2	1.2	1.0	0.95	0.71	2.7	1.1	0.31	0.12	0.54	0.50	0.73
4-4	1.7	1.2	1.1	0.76	0.75	2.8	1.3	0.36	0.10	0.55	0.48	0.77
4-5	1.9	1.3	0.96	0.99	0.71	2.7	1.3	0.35	0.13	0.57	0.51	0.73
5-1	1.7	1.3	0.75	1.0	0.63	2.4	1.2	0.37	0.27	0.57	0.57	0.67
5-2	1.8	1.2	0.58	0.66	0.58	1.9	1.1	0.36	0.43	0.54	0.63	0.63
5-3	1.9	1.2	1.0	1.0	0.72	2.7	1.4	0.34	0.14	0.55	0.50	0.74

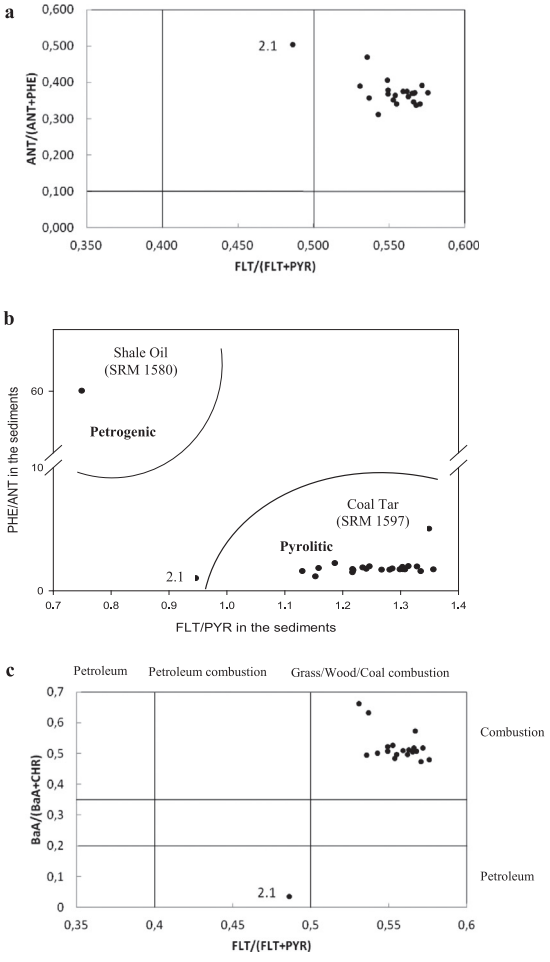

Fig. 4. Plots (a, b and c) of the diagnostic ratios calculated for the studied sediments. For b plot two matrices are reported on the graph to justify the petrogenic and pyrolytic area limitations (Wise et al., 1988).

only one factor, representing 98.46% of total variance. This is also sustained by the correlation of the individual PAHs, where all PAHs except IND and NAP showed a very strong correlation ($p < 0.05$) with $r \geq 0.94$, suggesting meanly a common source of these PAHs. A very strong correlation, $r = 0.99$, was also found between IND and NAP ($p < 0.05$).

The study evidenced a strong PAH contamination of the sediments of the entire Gulf of Pozzuoli, not only close to the Bagnoli plant. The amounts of FLT, PYR and BaP were higher than their respective ERL and ERM SGQs values: FLT 0.60–5.1 μg g^{-1}, PYR 0.66–2.6 μg g^{-1}, BaP 0.43–1.6 μg g^{-1}. These results indicate that the probability of a positive toxic effect is higher than 50% and hence organisms, especially fish in this location are in dangerous conditions. Outstanding levels of individual PAHs in all GoP were found with mean values higher than law limits from one hundred twenty seven fold (NAP) to seven hundred twenty five fold (BaP). This might have a strong environmental impact on the sea-bottom's ecological health.

Acknowledgements

We wish to thank the kind collaboration of the “Lega Navale di Pozzuoli”, the president, Silvio Luise, for giving us the use of the ship Antilia and the skipper Raffaele Donadio. We also wish to thank the Captaincy of the Port of Pozzuoli and the Lieutenant Commander Angelo Benedetto Gonnella in supporting the research and Anna Beltà for granulometric analysis.

References

Akyüz, M., Çabuk, H., 2010. Gaseparticle partitioning and seasonal variation of polycyclic aromatic hydrocarbons in the atmosphere of Zonguldak, Turkey. Sci. Total Environ. 408, 5550–5558.

Albanese, S., De Vivo, B., Lima, A., Cicchella, D., Civitillo, D., Cosenza, A., 2010. Geochemical baselines and risk assessment of the Bagnoli brownfield site coastal sea sediments (Naples, Italy). J. Geochem. Explor. 105, 19–33.

Barusseau, J.P., 1973. Evolution du Plateau continental rochelais (Golfe de Gascogne) au cours du Pléistocène terminal et de l'Holocène. Les processus actuels de la sédimentation. Thèse Univ. Bordeaux I (363 pp).

Baumard, P., Budzinski, H., Garrigues, P., Sorbe, J.C., Burgeot, T., Bellocq, J., 1998. Concentrations of PAHs (polycyclic aromatic hydrocarbons) in various marine organisms in relation to those in sediments and to trophic level. Mar. Pollut. Bull. 36,

951–960.
Belloni, S., 1969. Una tabella universale per eseguire granulometrie col metodo della sedimentazione unica o col metodo del densimetro di Casagrande modificato. Geologia Tecnica 16, 1281–1289.
Bergamin, L., Romano, E., Gabelllini, A., Ausili, A., Carboni, M.G., 2003. Chemical-physical and ecological characterisation in the environmental project of a polluted coastal area: the Bagnoli case study. Mediterr. Mar. Sci. 4, 05–20.
Blott, S.J., Pye, K., 2001. Gradistat: a grain size distribution and statistics package for the analysis of unconsolidated sediments. Earth Surf. Process. Landf. 26, 1237–1248.
Budzinski, H., Jones, I., Bellock, J., Pierard, C., Garrigues, P., 1997. Evaluation of sediment contamination by polycyclic aromatic hydrocarbons in the Gironde estuary. Mar. Chem. 58, 85–97.
Butler, J.D., Crossley, F., 1981. Reactivity of polycyclic aromatic hydrocarbons adsorbed on soot particles. Atmos. Environ. 15, 91–94.
Carrada, G.C., Hopkins, T.S., Bonaduce, G., Ianora, A., Marino, D., Modigh, M., Ribera d'Alcalà, A.M., Scotto Di Carlo, B., 1980. Variability in the hydrographic and biological features of the Gulf of Naples. Mar. Ecol. 1, 105–120.
Cerniglia, C.E., Heitkamp, M.A., 1989. In: Vanarasi, U. (Ed.), In Microbial Degradation of PAH in the Aquatic Environment. CRC Press, Boca Raton, FL, pp. 41–68.
Colantoni, P., 1972. Esalazioni vulcaniche sottomarine in relazione ai rilievi effettuati nell'area flegrea nel 1970–71. Quad. Ric. Sci. 83, 46–50.
Cortemiglia, G.C., 1978a. Valutazione quantitativa della variazione di fondale fra la foce del Magra e il porto di Marina di Carrara ed individuazione dei principali assi di transito del trasporto litoraneo. Mem. Soc. Geol. Ital. 19, 407–419.
Cortemiglia, G.C., 1978b. Le modificazioni dell'assetto strutturale del litorale di Lavagna quale fattore erosivo della spiaggia. Mem. Soc. Geol. Ital. 19, 369–380.
Cortemiglia, G.C., 1978c. Applicazione di curve di isodensità carbonatica per classi granulometriche modali nello studio della dinamica litorale. Mem. Soc. Geol. Ital. 19, 321–330.
Dahle, S., Savinov, V.M., Matishov, G.G., Evenset, A., Næs, K., 2003. Polycyclic aromatic hydrocarbons (PAHs) in bottom sediments of the Kara Sea shelf, Gulf of Ob and Yenisei Bay. Sci. Total Environ. 306, 57–71.
Damiani, V., Baudo, R., De Rosa, S., De Simone, R., Ferretti, O., Lzzo, G., Serena, F., 1987. A case study: bay of Pozzuoli (Gulf of Naples, Italy). Hydrobiology 149, 201–211.
De La Torre-Roche, R.J., Lee, W.Y., Campos-Díaz, S.I., 2009. Soil-borne polycyclic aromatic hydrocarbons in El Paso, Texas: analysis of a potential problem in the United States/Mexico border region. J. Hazard. Mater. 163, 946–958.
De Maio, A., Moretti, M., Surone, E., Spezia, G., Voitaggio, M., 1982. Circolazione costiera. Analisi dinamica e idrologica di una situazione osservata nel Golfo di Napoli. Convegno Risorse Biologiche e Inquinamento Marino del P.F. Oceanografia e Fondi Marinipp. 609–624.
De Pippo, T., 1989. Coastal dynamics and sedimentary transit axes on the Volturno River Mouth (Campania, Italy). Rend. Acc. Sci. Fis e Mat., Soc. Naz. Sci. Lett. Art. Napolipp. 27–45 (serie IV, LV).
De Pippo, T., Donadio, C., Pennetta, M., Terlizzi, F., Vecchione, C., Vegliante, M., 2002. Seabed morphology and pollution along the Bagnoli coast (Naples, Italy): a hypothesis of environmental restoration. Mar. Ecol. 23, 154–168.
De Pippo, T., Donadio, C., Pennetta, M., 2004. Morphological control on sediment dispersal along the southern Tyrrhenian coasts (Italy). Geol. Romana 37, 113–121.
Folk, R.L., Ward, W.C., 1957. Brazos River bar: a study in the significance of grain size parameters. J. Sediment. Petrol. 27, 3–26.
Hwang, H.M., Foster, G.D., 2006. Characterization of polycyclic aromatic hydrocarbons in urban stormwater runoff flowing into the tidal Anacostia River, Washington, DC, USA. Environ. Pollut. 140, 416–426.
ISPRA, 2009. Registro Nazionale INES - Inventario Nazionale delle Emissioni e delle loro Sorgenti.
Lake, J.L., Norwood, C., Dimock, C., Bowen, R., 1979. Origins of polycyclic aromatic hydrocarbons in estuarine sediments. Geochim. Cosmochim. Acta 43, 1847–1854.
Law, R.J., Dawes, V.J., Woodhead, R.J., Matthiessen, P., 1997. Polycyclic aromatic hydrocarbons (PAH) in sea water around England and Wales. Mar. Pollut. Bull. 34, 306–322.
Lehr, R.E., Jerina, D.M., 1977. Metabolic activation of polycyclic aromatic hydrocarbons. Arch. Toxicol. 39, 1–6.
Long, B., 1975. Le littoral Nord-Ouest de l'Ile de Ré (Charent maritime). Les processus dynamiques de la sédimentation et l'évolution côtière résultante. Thèse 3e Cycle Univ. Toulouse III (236 pp.).
Long, E.R., MacDonald, D.D., Smith, S.L., Calder, F.D., 1995. Incidence of adverse biological effects within ranges of chemical concentrations in marine and estuarine sediments. Environ. Manag. 19, 81–97.
Mangoni, O., Aiello, G., Balbi, S., Barra, D., Bolinesi, F., Donadio, C., Ferrara, L., Guida, M., Parisi, R., Pennetta, M., Trifuoggi, M., Arienzo, M., 2016. A multidisciplinary approach for the characterization of the coastal marine ecosystems of Monte Di Procida (Campania, Italy). Mar. Pollut. Bull. 112, 443–451.
Mill, T., Mabey, W.R., Lan, B.Y., Baraze, A., 1981. Photolysis of polycyclic aromatic hydrocarbons in water. Chemosphere 10, 1281–1290.
Nasher, E., Heng, L.Y., Zakaria, Z., Surif, S., 2013. Concentrations and sources of polycyclic aromatic hydrocarbons in the seawater around Langkawi Island, Malaysia. J. Chem. http://dx.doi.org/10.1155/2013/975781.
Parlanti, E., 1990. Utilisation des hydrocarbures comme traceurs d'origine de la matière organique sédimentaire en milieu marin. In: Etude du Golfe du Lyon et du Golfe de Gascogne (Programme Ecomarge). University Bordeaux I, Bordeaux, France PhD thèses Nr 495. (289 pp).
Patacca, E., Sartori, R., Scandone, P., 1990. Tyrrhenian basin and Apenninic arcs: kinematic relations since Late Tortonian times. Mem. Soc. Geol. Ital. 45, 425–451.
Pauc, H., 1973. Les modes granulométriques et la phases de mise en place du recouvrement sédimentaire du plateau continental au sud de l'Ile du Levant. Ann. Hydrogr. 5.
Pennetta, M., Valente, A., Abate, D., Boudillon, G., De Pippo, T., Leone, M., Terlizzi, F., 1998. Influenza della morfologia costiera sulla circolazione e sedimentazione sulla piattaforma continentale campano-laziale tra Gaeta e Cuma (Italia meridionale). Boll. Soc. Geol. Ital. 117, 281–295.
Pies, C., Hoffmann, B., Petrowsky, J., Yang, Y., Ternes, T.A., Hofmann, T., 2008. Characterization and source identification of polycyclic aromatic hydrocarbons (PAHs) in river bank soils. Chemosphere 72, 1594–1601.
Ravindra, K., Wauters, E., Van Grieken, R., 2008a. Variation in particulate PAHs levels and their relation with the transboundary movement of the air masses. Sci. Total Environ. 396, 100–110.
Ravindra, K., Sokhi, R., Van Grieken, R., 2008b. Atmospheric polycyclic aromatic hydrocarbons: source attribution, emission factors and regulation. Atmos. Environ. http://dx.doi.org/10.1016/j.atmosenv.2007.12.010.
Readman, J.W., Mantoura, R.F.C., Rhead, M.M., 1984. The physical-chemical speciation of polycyclic aromatic hydrocarbons (PAH) in aquatic systems. Fresenius' Z. Anal. Chem. 319, 126–131.
Richir, J., Salivas-Decaux, M., Lafabrie, C., Lopez y Royo, C., Gobert, S., Pergent, G., 2015. Bioassessment of trace element contamination of Mediterranean coastal waters using the seagrass *Posidonia oceanica*. J. Environ. Manag. 51, 486–499.
Romano, E., Bergamin, L., Ausili, A., Pierfranceschi, G., Maggi, C., Sesta, G., Gabellini, M., 2009. The impact of the Bagnoli industrial site (Naples, Italy) on sea-bottom environment. Chemical and textural features of sediments and the related response of benthic foraminifera. Mar. Pollut. Bull. 59, 245–256.
Sgrosso, I., 1998. Possibile evoluzione cinematica miocenica nell'orogene centro-sudappenninico. Boll. Soc. Geol. Ital. 117, 679–724.
Sharp, W.E., Nardi, G., 1987. A study of the heavy metal pollution in the bottom sediments at Porto di Bagnoli (Naples), Italy. J. Geochem. Explor. 29, 49–73.
Sicre, M.A., Marty, J.C., Saliot, A., 1987. Aliphatic and aromatic hydrocarbons in different sized aerosols over the Mediterranean sea: occurrence and origin. Atmos. Environ. 21, 2247–2259.
Simpson, C.D., Mosi, A.A., Cullen, W.R., Reimer, K.J., 1996. Composition and distribution of polycyclic aromatic hydrocarbon contamination in surficial marine sediments from Kitimat Harbor, Canada. Sci. Total Environ. 181, 265–278.
Smith, J.N., Levy, E.M., 1990. Geochronology of polycyclic aromatic hydrocarbon contamination in sediments of the Saguenay Fjord. Environ. Sci. Technol. 24, 874–879.
Soclo, H., 1986. Etude de la distribution des hydrocarbures aromatiques polycycliques dans les sédiments marins récents, identification des sources. Ph.D. Thesis University Bordeaux I, Bordeaux, France (158 pp.).
Soclo, H.H., Garrigues, P., Ewald, M., 2000. Origin of polycyclic aromatic hydrocarbons (PAHs) in coastal marine sediments: case studies in Cotonou (Benin) and Aquitaine (France) areas. Mar. Pollut. Bull. 40, 387–396.
Somma, R., Iuliano, S., Matano, F., Molisso, F., Passaro, S., Sacchi, M., Troise, C., De Natale, G., 2016. High-resolution morpho-bathymetry of Pozzuoli Bay, southern Italy. J. Maps 12, 222–230.
Tobiszewski, M., Namiesnik, J., 2012. PAH diagnostic ratios for the identification of pollution emission sources. Environ. Pollut. 162, 110–119.
Wang, R.W., Liu, G.J, Zhang, J.M., Chou, C.L., Liu, J., 2010. The abundances of polycyclic aromatic hydrocarbons (PAHs) in fourteen Chinese and U.S. coals and their relation to coal ranks and weathering. Energy Fuel 24, 6061–6066.
Wise, S.A., Hilpert, L.R., Rebbert, R.E., Sander, L.C., Schantz, M.M., Chesler, S.N., May, W.E., 1988. Fresenius' Z. Anal. Chem. 332, 573–582.
Yan, B., Benedict, L., Chaky, D.A., Bopp, R.F., Abrajano, T.A., 2004. Levels and patterns of PAH distribution in sediments from New York/New Jersey Harbor Complex. Northeast. Geol. Environ. Sci. 26, 113–122.
Yunker, M.B., Macdonald, R.W., Vingarzan, R., Mitchell, R.H., Goyette, D., Sylvestre, S., 2002. PAHs in the Fraser River basin: a critical appraisal of PAH ratios as indicators of PAH source and composition. Org. Geochem. 33, 489–515.
Zakaria, M.P., Azril Mahat, A., 2006. Distribution of Polycyclic aromatic hydrocarbon (PAHs) in sediments in the Langat estuary. Costal Mar. Sci. 30, 387–395.